

Accepted Manuscript

XAFS study of metal chelates of phenylazo derivatives of Schiff bases

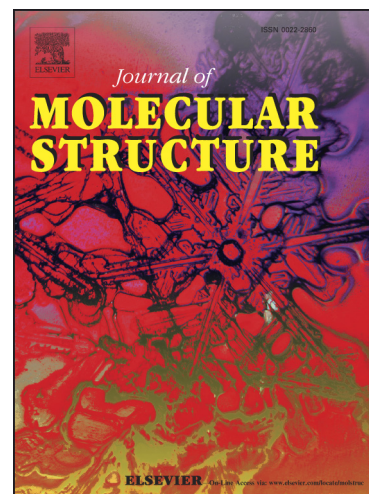
Anatolii S. Burlov, Sergey A. Mashchenko, Valery G. Vlasenko, Yan V. Zubavichus, Ali I. Uraev, Konstantin A. Lyssenko, Sergei I. Levchenkov, Igor S. Vasilchenko, Dmitrii A. Garnovskii, Gennadii S. Borodkin

PII: S0022-2860(13)01030-2

DOI: <http://dx.doi.org/10.1016/j.molstruc.2013.12.007>

Reference: MOLSTR 20196

To appear in: *Journal of Molecular Structure*



Please cite this article as: A.S. Burlov, S.A. Mashchenko, V.G. Vlasenko, Y.V. Zubavichus, A.I. Uraev, K.A. Lyssenko, S.I. Levchenkov, I.S. Vasilchenko, D.A. Garnovskii, G.S. Borodkin, XAFS study of metal chelates of phenylazo derivatives of Schiff bases, *Journal of Molecular Structure* (2013), doi: <http://dx.doi.org/10.1016/j.molstruc.2013.12.007>

This is a PDF file of an unedited manuscript that has been accepted for publication. As a service to our customers we are providing this early version of the manuscript. The manuscript will undergo copyediting, typesetting, and review of the resulting proof before it is published in its final form. Please note that during the production process errors may be discovered which could affect the content, and all legal disclaimers that apply to the journal pertain.

XAFS study of metal chelates of phenylazo derivatives of Schiff bases

Anatolii S. Burlov ^a, Sergey A. Mashchenko ^a, Valery G. Vlasenko ^b,
Yan V. Zubavichus ^c, Ali I. Uraev ^a, Konstantin A. Lyssenko ^d,
Sergei I. Levchenkov ^e, Igor S. Vasilchenko ^{a,1}, Dmitrii A. Garnovskii ^{a,e},
Gennadii S. Borodkin ^a

^a Institute of Physical and Organic Chemistry of Southern Federal University, Stachki ave. 194/2, Rostov-on-Don, 344090 Russian Federation, e-mail: garn@ipoc.rsu.ru

^b Institute of Physics of Southern Federal University, Stachki ave. 194, Rostov-on-Don, 344090 Russian Federation

^c National Research Centre "Kurchatov Institute", Akademik Kurchatov sq. 1, Moscow, 123182 Russian Federation

^d A.N. Nesmeyanov Institute of Organoelement Compounds, Russian Academy of Sciences, Vavilova str. 28, Moscow, 119991 Russian Federation

^e Southern Scientific Center of Russian Academy of Sciences, Chekhova str. 41, 344006 Rostov-on-Don, Russian Federation

A B S T R A C T

The Schiff base derived from *o*-tosylaminobenzaldehyde and *p*-aminoazobenzene and its metal chelates (Co²⁺, Ni²⁺, Cu²⁺, and Zn²⁺) have been synthesized and investigated (IR, ¹H NMR, XANES, EXAFS spectroscopy, X-ray diffraction, magnetic measurements). It was found that the azomethine exists in the amino-imine tautomeric form both in solutions and solid state. XAFS investigations reveal that the complexes

¹ Author to whom correspondence should be addressed

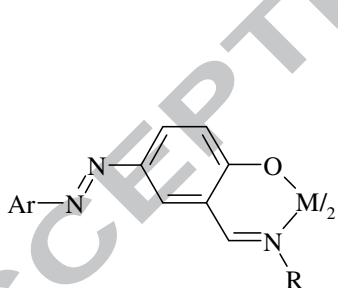
adopt either distorted tetrahedral or octahedral (due to additional coordination of oxygen atoms of the tosylamino group) ligand environment.

Keywords: azophenyl Schiff bases; 3d-metals; mononuclear complexes; *N,N*-coordination, XAFS, X-ray diffraction

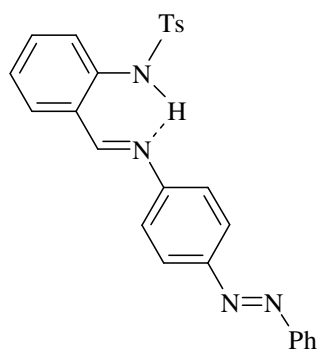
1. Introduction

Schiff bases are among the most important ligands of the modern coordination chemistry [1-12] since their complex-forming activity makes them attractive for the design of novel multifunctional materials, *e.g.*, molecular magnets [13-16], luminophores [17, 18], and bioactive chelates [19, 20].

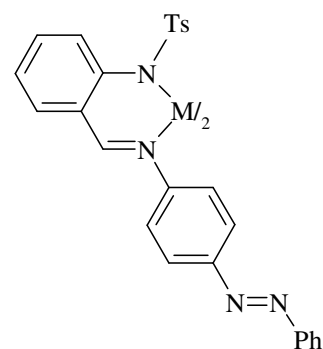
Coordination compounds of Schiff bases bearing an azo group are represented by complexes of ligands containing an Ar-N=N- fragment in the aldehyde moiety, which are essentially chelates of azomethines of arylazosalicylaldehyde **1** [8, 15, 21, 22-24].



1



2: Ts = -SO₂C₆H₄CH₃-*p*



3: M = Co (a), Ni (b),
Cu (c), Zn (d)

Metallocomplexes of azomethines containing arylazo-group in the amine moiety presented only by chelates on the base of ligands with N₂O₂ donor atoms set [25, 26].

So synthesis and investigation of the same complexes with N₄ donor environment is a matter of interest.

We have synthesized and investigated Schiff base **2** with an azo group within the amine moiety and its metal complexes **3**, and have studied of influence of the character of such substituent on their structural and magnetic characteristics.

2. Experimental

2.1. Materials

All solvents, metal acetates and organic precursors were purchased from Aesar, Lancaster.

2.2. Synthesis of the azoderivative 2

A hot solution of 1.97 g (0.01 mol) of 4-aminoazobenzene in 30 ml of methanol was added to a hot solution of 2.75 g (0.01 mol) of 2-tosylaminobenzaldehyde in 20 ml of the same solvent. Resulting mixture was refluxed for 1 h. Precipitate formed after cooling to the room temperature was filtered off, washed with cool methanol, dried in air and recrystallized from the chloroform-methanol mixture (1:2). Obtained crystals were available for X-ray structural investigations. Red-orange crystals, m.p. 204-205 °C, yield 84 %. Found, %: C, 68.75; H, 4.95; N, 12.41. Calculated for C₂₆H₂₂N₄O₂S, %: C, 68.71; H, 4.88; N, 12.32. NMR ¹H (CDCl₃), δ (ppm): 2.36 (3H, s, CH₃), 7.11 (1H, t, C-H_{Ar}), 7.21 (1H, d, C-H_{Ar}), 7.23 (1H, d, C-H_{Ar}), 7.36-7.57 (7H, m, C-H_{Ar}), 7.70 (1H, d, C-H_{Ar}), 7.79 (1H, d, C-H_{Ar}), 7.80 (1H, d, C-H_{Ar}), 7.94 (1H, d, C-H_{Ar}), 7.96 (1H, d, C-H_{Ar}), 8.01 (1H, d, C-H_{Ar}), 8.04 (1H, d, C-H_{Ar}), 8.56 (1H, s, HC=N), 12.75 (1H, s, NH).

IR spectrum, ν (cm^{-1}): 2700-3100 (br, NH), 1617 (s, C=N), 1334 (vs, SO₂, as), 1152 (vs, SO₂, sym).

2.3. Synthesis of the complexes 3a-d

All complexes have been obtained according to the below common method. A hot solution of 0.001 mol of the acetate of the corresponding *d*-metal in 10 ml of methanol was added to a hot solution of 0.91 g (0.001 mol) of azomethine **2** in 50 ml of the same solvent. The resulting mixture was refluxed for 1 h and cooled for the room temperature. Precipitates of complexes was filtered off, washed with hot methanol and dried *in vacuo*.

3a. Red-brown powder, m.p. 241-242 °C, yield 98 %. Found, %: C, 64.68; H, 4.42; N, 11.58. Calculated for C₅₂H₄₂N₈O₄S₂Co, %: C, 64.66; H, 4.38; N, 11.60. IR spectrum, ν (cm^{-1}): 1604 (s, C=N), 1258 (vs, SO₂, as), 1134 (vs, SO₂, sym). $\mu_{\text{eff}} = 4.29$ BM (294 K).

3b. Brown powder, m.p. > 250 °C, yield 88 %. Found, %: C, 64.65; H, 4.40; N, 11.65. Calculated for C₅₂H₄₂N₈O₄S₂Ni, %: C, 64.68; H, 4.38; N, 11.60. IR spectrum, ν (cm^{-1}): 1603 (s, C=N), 1257 (vs, SO₂, as), 1125 (vs, SO₂, sym). $\mu_{\text{eff}} = 3.89$ BM (294 K).

3c. Dark-brown powder, m.p. > 250 °C, yield 85 %. Found, %: C, 64.42; H, 4.38; N, 11.60. Calculated for C₅₂H₄₂N₈O₄S₂Cu, %: C, 64.35; H, 4.36; N, 11.54. IR spectrum, ν (cm^{-1}): 1606 (s, C=N), 1261 (vs, SO₂, as), 1130 (vs, SO₂, sym). $\mu_{\text{eff}} = 1.74$ BM (294 K).

3d. Orange powder, m.p. > 250 °C, yield 75 %. Found, %: C, 64.34; H, 4.30; N, 11.62. Calculated for C₅₂H₄₂N₈O₄S₂Zn, %: C, 64.23; H, 4.35; N, 11.52. NMR ¹H (DMSO-*d*₆), δ (ppm): 2.25 (6H, s, CH₃), 6.70-7.87 (34H, m, C-H_{Ar}), 8.87 (1H, s, HC=N). IR spectrum, ν (cm^{-1}): 1607 (s, C=N), 1261 (vs, SO₂, as), 1133 (vs, SO₂, sym).

2.4. Physical measurements

C, H, and N analyses were performed with a Carlo Erba Instruments TCM 480 analyzer. IR spectra of powder samples and as KBr pellets were recorded using a Varian Excalibur-3100 FT-IR spectrophotometer. ^1H NMR spectra (in CDCl_3 for organic derivative and in $\text{DMSO}-d_6$ for complexes) were measured with a Bruker Avance-600 spectrometer (600 MHz) with the signal of residual ^1H in solvent as the internal standard.

2.5. X-ray diffraction

Orange-red crystals of *N*-(4-phenylazo)phenyl-(2-tosylamino)benzaldimine $\text{C}_{26}\text{H}_{22}\text{N}_4\text{O}_2\text{S}$ (**2**) are monoclinic: $a = 11.7576(12)$ Å, $b = 11.7288(12)$ Å, $c = 16.7054(17)$ Å, $\alpha = 90^\circ$, $\beta = 100.899(5)^\circ$, $\gamma = 90^\circ$, $V = 2262.2(4)$ Å³, $M = 454.54$, $F(0\ 0\ 0) = 952$, $\rho_{\text{calcd}} = 1.318$ g cm⁻³, $\mu = 0.175$ g cm⁻¹, $Z = 4$, space group $P\ 21/c$, $T = 120(2)$ K.

Experimental data for **2** were obtained with an Bruker SMART 1000 diffractometer (λ Mo-K α , graphite monochromator, $\theta/2\theta$ -scanning, $\theta_{\text{max}} = 28^\circ$). Intensities of 874 reflections were measured.

The structure of this compound was determined by direct methods (SHELXS PLUS) [27], refined by full-matrix least-squares on F^2 in the anisotropic approximation for all non-hydrogen atoms. Hydrogens were placed in the calculated positions and refined according to the riding model with fixed Debye factors of $U_{\text{H}} = 0.08$ Å².

The final fitting parameters for **2** are: $R_1 = 0.0593$, $wR_2 = 0.1311$ on 874 reflections with $F_o \geq 2\sigma(F_o)$, $R_1 = 0.1021$, $wR_2 = 0.1565$ on all reflections, 299 variable parameters, index range: $-15 \leq h \leq 15$, $-15 \leq k \leq 15$, $-22 \leq l \leq 22$, goodness-of-fit = 1.004, residual electronic density $\Delta\rho_{\text{min}} = -0.284$, $\Delta\rho_{\text{max}} = 0.460$ e Å⁻³.

2.6. XAS measurements and analysis

Ni *K*-, Co *K*- and Cu *K*-edges EXAFS spectra for the complexes were obtained at the Station K1.3b "Structural Materials Science" of the Kurchatov Center of Synchrotron Radiation and Nanotechnology (KCSRNT, Moscow, Russia) [28]. The storage ring with electron beam energy of 2.5 GeV and a current of 70–90 mA was used as the source of radiation. All the spectra were recorded in the transmission mode using a channel-cut Si(111) monochromator and two N₂/Ar-filled ionization chambers as detectors. EXAFS data ($\chi_{\text{exp}}(k)$) were analyzed using the IFEFFIT data analysis package [29]. EXAFS data reduction used standard procedures for the pre-edge subtraction and spline background removal.

The radial pair distribution functions around the Ni, Co, and Cu ions were obtained by the Fourier transformation of the k^3 -weighted EXAFS functions over the ranges of photoelectron wave numbers 2.4–12.5 Å⁻¹. The structural parameters, including interatomic distances (*R*), coordination numbers (*CN*) and the distance mean-square deviations also known as Debye–Waller factors (σ^2), were found by the non-linear fit of theoretical spectra to experimental ones. The experimental data were simulated using the theoretical EXAFS amplitude and phase functions, which were calculated using the program FEFF7 [30]. The amplitude reduction factor S_0^2 , and the threshold energy offset ΔE_0 were calibrated by fitting EXAFS data for model compounds. The amplitude reduction factor S_0^2 was found equal to 0.9 in all cases.

The quality of fits was estimated from discrepancy factors between the experimental and simulated functions (*Q*-factor).

$$Q(\%) = \frac{\sum [k\chi_{\text{exp}}(k) - k\chi_{\text{th}}(k)]^2}{\sum [k\chi_{\text{exp}}(k)]^2} \cdot 100\%$$

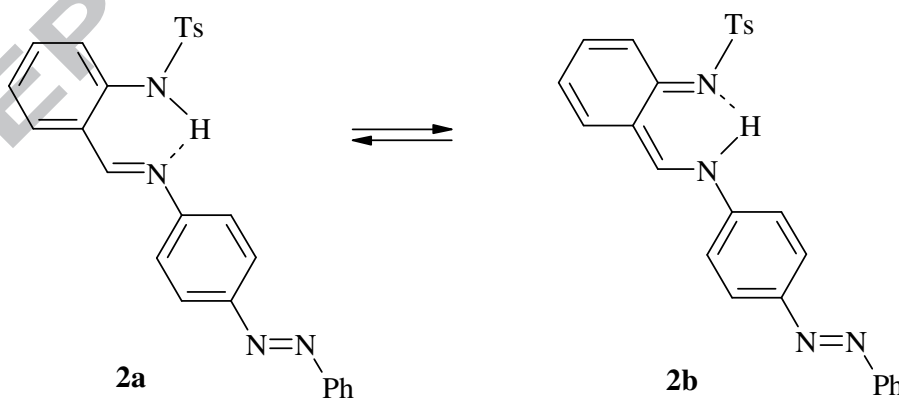
2.7. Magnetic susceptibility measurements

The magnetic susceptibility of the sample has been measured by the Faraday method at 294 K. Hg[Co(NCS)₄] was used as a reference sample for settings of the equipment.

3. Results and discussion

3.1. Structure of the ligand **2**

IR (ν NH 2700-3100 cm^{-1} , ν C=N 1617 cm^{-1}) and NMR ¹H (δ HC=N 8.56 ppm, δ NH 12.75 ppm) data reveal that the compound **2** favorable exists as amino-imine tautomer **2a** in solution and as a solids.



The same structure (Fig. 1) has been found for the imine **2** in crystal that is in agreement with literatural data for other azomethine derivatives of 2-

tosylaminobenzaldehyde [31-34]. The broad peak at 2700-3100 cm^{-1} in the IR spectrum of **2** may be attributed to the stretching of N-H group involved in the strong hydrogen bond. Among other IR spectral data point the bands at 1152 and 1334 cm^{-1} corresponding to the *sym* and *asym* vibrations of SO_2 group which are important for the discussion of the structure of coordination compounds [35-38].

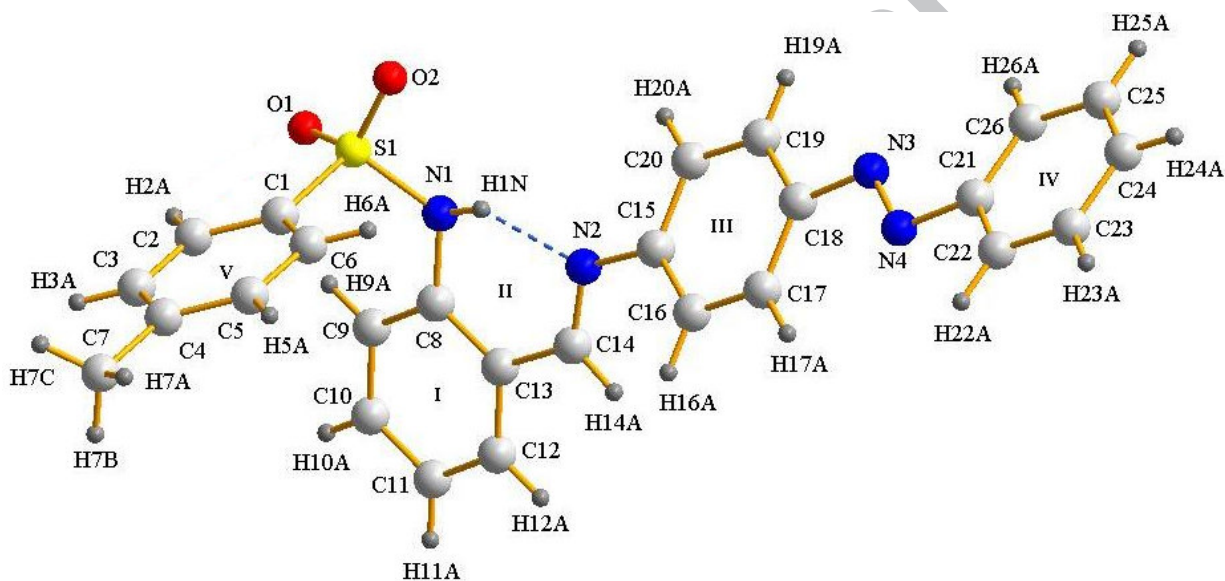


Fig. 1. Structure of the azomethine **2**. Selected bond distances (\AA): S(1)-O(1) 1.4282(18), S(1)-O(2) 1.4349(18), S(1)-N(1) 1.630(2), S(1)-C(1) 1.759(2), N(1)-C(8) 1.412(3), N(1)-H(1)N 0.9121, N(2)-C(14) 1.279(3), N(2)-C(15) 1.413(3), N(3)-N(4) 1.261(3), N(3)-C(18) 1.422(3), N(4)-C(21) 1.425(3); and valence angles ($^\circ$): O(1)S(1)O(2) 119.43(11), O(1)S(1)N(1) 109.91(11), O(2)S(1)N(1) 104.06(10), O(1)S(1)C(1) 107.02(11), O(2)S(1)C(1) 109.19(12), N(1)S(1)C(1) 106.59(11), C(8)N(1)S(1) 125.30(16), C(8)N(1)H(1)N 111.5, S(1)N(1)H(1)N 108.7, C(14)N(2)C(15) 121.5(2), N(4)N(3)C(18) 114.2(2), N(3)N(4)C(21) 113.7(2).

Bond distances C(8)-N(1) (1.412(3) \AA) and C(14)-N(2) (1.280(3) \AA) correspond to amino-imine form of compound **2** in the solid state [39]. This form stabilized in the

crystal by almost strong hydrogen bond N(1)–H(1N)···N(2) (Table 1) forming six-membered cycle N(1)H(1N)N(3)C(14)C(13)C(8) (fragment II - see Fig. 1).

Table 1

Characteristics of hydrogen bonds in the crystal of compound **2**.

D–H···A	D– H, Å	H...A, Å	D...A, Å	∠DHA, deg.
N(1)–H(1N)···N(2)	0.91	1.88	2.656(3)	142
C(2)–H(2A)···O(1)	0.95	2.49	2.872(3)	104
C(9)–H(9A)···O(1)	0.95	2.51	3.164(3)	126
C(6)–H(6A)···O(1) ⁱ	0.95	2.35	3.216(3)	151
C(25)– H(25A)···O(2) ⁱⁱ	0.95	2.47	3.234(3)	138

Crystallographic sites: (i) 2–x, 1–y, 1–z; (ii) 1–x, 1/2+y, 1/2–z.

The X-ray structural data reveal that the central part of the molecule is almost planar - dihedral angle between cycles C(8)C(9)C(10)C(11)C(12)C(13) (I) and II is 2.09° (Fig. 1). Hydrogen atom H(1N) deviates from N(1)C(8)C(14)C(13)N(2) plane on 0.140 Å. Cycle III is turned clockwise (looking from the cycle IV) relative cycle I on 31.37°, bond N(3)–N(4) forms angles with planes III and IV in 2.609(97) and 8.099(109)° respectively, so this moiety of the molecule has a helix-like form.

The planes of phenyl rings C(15)C(16)C(17)C(18)C(19)C(20) (III) and C(21)C(22)C(23)C(24)C(25)C(26) (IV) linked by the azo group are partially non-coplanar (dihedral angle between mean planes is equal to 19.51°).

Valence angles at the atoms N(1) and S(1) correspond to their sp^3 hybridization.

Atom O(1) forms two short contacts which may be assigned to intramolecular C–H \cdots O hydrogen bonds [40]. Atoms O(1) and O(2) participate in the intermolecular C–H \cdots O hydrogen bonds (Table 1). Any π -stacking interactions in the crystal are not found.

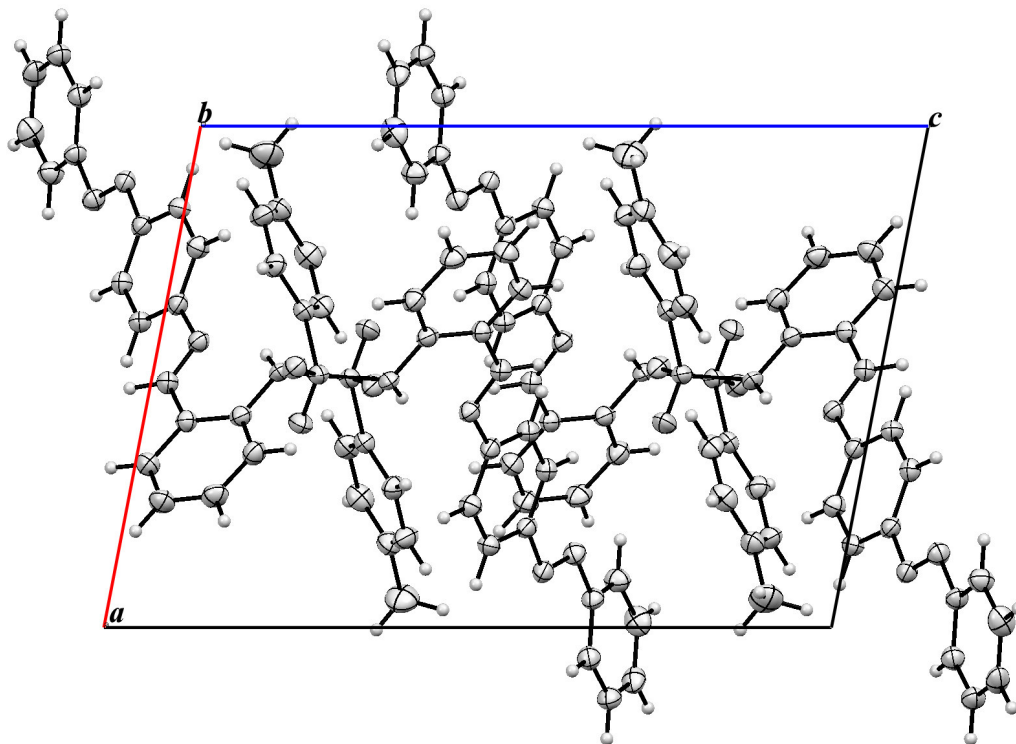


Fig. 2. View of crystal packing of **2** along *b* crystallographic axis.

3.2. Characterization of the complexes

Formation of the bis-chelates **3a-d** as result of the coupling ligating Schiff base **2** with acetates of bivalent *d*-metals (method of direct interaction [2]) is supported by the results of element analysis (composition ML_2 , where LH – compound **2**) and IR, 1H NMR, XAFS spectroscopy and magnetochemical (for chelates **3a-c**) measurements.

3.2.1. IR and ^1H NMR spectra

IR spectra of the complexes **3a-d** demonstrate disappearing of the broad band of the NH stretching ($2700\text{-}3100\text{ cm}^{-1}$) as compared with the spectrum of the compound **2** that may be relevant to the substitution of the proton by the metal ion. Low frequency shifts of the C=N stretching band in the IR spectra of the complexes **3a-d** (by $10\text{-}13\text{ cm}^{-1}$) as compared with the spectrum of the azomethine **2**) may point [13, 35] to the coordination of the nitrogen atom of this group to the metal and formation of the chelate structure. Analogous behaviour of the stretching bands $\text{SO}_2(\text{as})$ (by the $73\text{-}76\text{ cm}^{-1}$) and $\text{SO}_2(\text{sym})$ (by the $19\text{-}27\text{ cm}^{-1}$) may be caused by coordination interactions of metal with oxygen atoms of the above group [41]. NMR ^1H data zinc for complex confirm above conclusion – disappearing the proton signal of the NH group (12.75 ppm), upfield shift of the proton signal of HC=N group (8.87 ppm in the spectrum of compound **3d** *vis* 8.56 ppm in the spectrum of **2**).

3.2.2. Magnetochemical investigation

Magnetic susceptibility measurements results in the temperature range of 77-294 K show that the magnitudes of μ_{eff} (4.29 – **3a**, 3.89 – **3b**, 1.74 – **3c**) are practically independently on the temperature. These values may be relevant to the tetrahedral or distorted-octahedral (due to the coordination of the oxygen atoms of SO_2 groups to the metal) coordination geometry.

3.2.3. XAS spectroscopy

X-ray absorption spectroscopy (XAS) was used to investigate the structure of metal complexes **3**. While extended X-ray absorption fine structure (EXAFS) analysis provides information on the types of coordinated atoms and very accurate first-shell metal-ligand distances, it determines the coordination numbers with a lower accuracy and generally gives little or no information on the coordination site 3D geometry. However, complementary information can be obtained from the near-edge region of XAS spectra, *i.e.*, XANES.

K-edge XAS spectra of first-row transition metals typically have a weak pre-edge feature at an energy 10 eV below the absorption edge. This feature is traditionally assigned to a $1s \rightarrow 3d$ transition [42, 43]. For complexes in a centrosymmetric environment, the $1s \rightarrow 3d$ transition is strictly forbidden by electric dipole selection rules due to parity considerations. However, a very weak pre-edge feature is still experimentally observed for such complexes due to the electric quadrupole contribution. Since the electric quadrupole-coupled mechanism is so much weaker than the electric dipole-coupled mechanism, only a few percent of 4p mixing into the 3d orbitals can make a significant effect on the intensity of the $1s \rightarrow 3d$ pre-edge feature [44]. Complexes in a noncentrosymmetric environment are expected to exhibit a more intense pre-edge feature than centrosymmetric complexes. This increase in intensity has been attributed to the 4p-3d metal orbital mixing, which provides some electric-dipole-allowed $1s \rightarrow 4p$ character to the transition. Thereby, the energy, intensity, and splitting of the $1s \rightarrow 3d$ pre-edge feature are extremely sensitive to the chemical and structural local environment of the metal site in complexes.

The XAS edge spectra for Cu, Ni, and Co metal complexes **3** are shown in Figures 3-5. An expanded view of the $1s \rightarrow 3d$ pre-edge region and the first derivative of the K-edge of these metal complexes **3** are shown as insets in Figures 3-5. All three complexes have relatively intense pre-edge features. Such an intensity of the pre-edge features of the complexes are due to $1s \rightarrow 3d$ electronic transitions originated from both the electric quadrupole and 3d-4p mixing (electric dipole) mechanisms, and thus is an indication of a noncentrosymmetric environment around the metal ions in these complexes.

The Cu, Ni, and Co K-edge XANES spectra and their first derivatives for metal complexes **3** and model compounds are shown in Figures 3-5. XANES is generated by the photoelectron transition from inner orbitals to upper unoccupied ones of absorbing atoms $1s \rightarrow 4s$ and $1s \rightarrow 4p$ [45-47]. A spectral feature of XANES region depends upon oxidation state of absorbing atoms, site symmetry, surrounding ligands and nature of bonding.

The theoretical simulation of XANES spectra at the Cu, Ni and Co K-edges for metal complexes **3** was performed using the self-consistent full multiple-scattering approach as implemented in the FEFF8.2 code [48, 49]. Phase shifts of the photoelectron were calculated in the framework of the self-consistent crystal muffin-tin (MT) potential scheme with a 15% overlap of the MT spheres. The Hedin-Lundqvist exchange-correlation potential neglecting the presence of a core hole gave the best results. We performed a search for structural models with coordination site geometries similar to those in each of metal complexes **3** in the Cambridge Structural Database (CSD). More than twenty models were simulated for each complex, and the theoretical curves along with their first derivatives were compared to the experimental ones.

It is clearly seen that the main peculiarities of the experimental XANES spectra and their first derivatives are reproduced in detail in the simulated spectra. Some disagreement is observed only in the pre-edge region, where absorption peaks are shifted by several eV towards higher energies, as it can be seen from Fig. 3-5. As it has been suggested in [50], the reason for the disagreement lies within the drawbacks of muffin-tin approximation as regards of the exchange potentials employed in FEFF8 code. This approximation is sufficiently precise for solid state (most inorganic crystals), but may result in significant deviations of theoretical and experimental spectra of molecular crystals of metal complexes characterized by the presence of large cavities, which are not treated adequately within the muffin-tin approximation.

The interligand tilt angle is one of the key quantitative characteristics of coordination site geometry in metal complexes **3**. This tilt angle Δ is defined as an angle between the planes going through the M-N1-N2 and M-N3-N4 atoms. Values of the tilt angles for possible coordination environments are listed in Table 2. This angle Δ

characterizes the transformation from tetrahedral to planar coordination, when it changes from to 90° or 0° . It is seen from Table 2 that the lowest value of the tilt angle is obtained for **3b**, which shows that the coordination in this compound is planar-like. It should be noted that in this case the possible additional coordination of oxygen atoms of tosylamine fragments was not taken into account. In this case the resulting symmetry of the coordination site may be described as a more-or-less tetragonally distorted octahedron, for example.

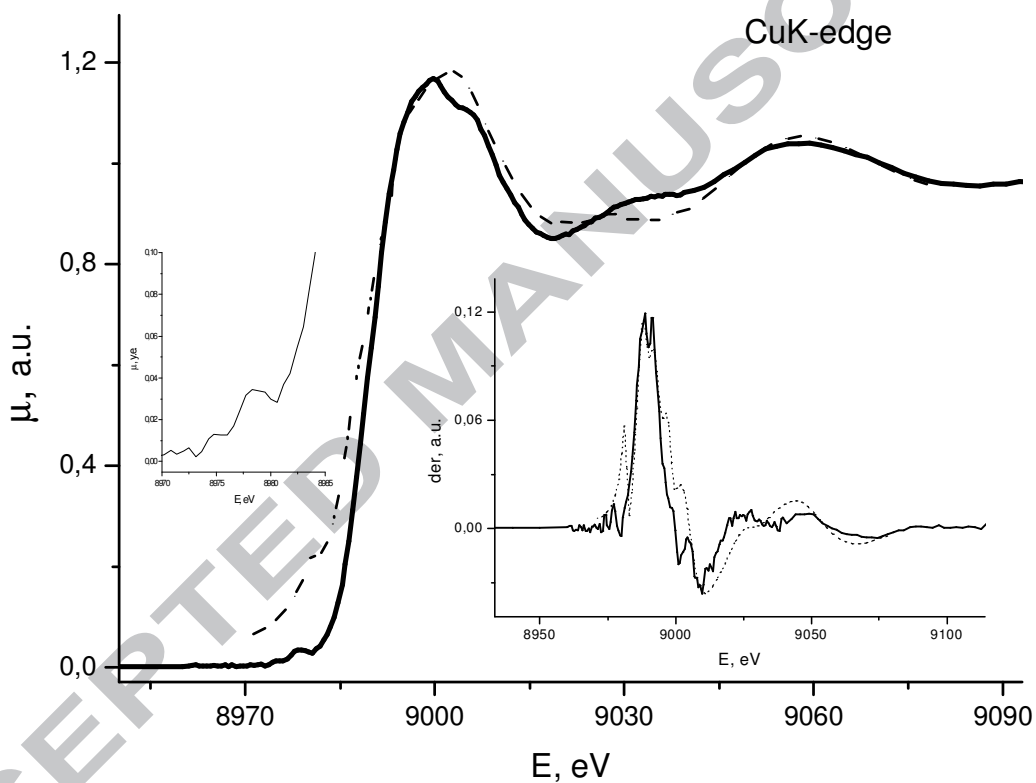


Fig. 3. The experimental Cu *K*-edge XAS spectrum (solid line) of **3c** complex and calculated Cu*K*-edge (dashed line) XAS spectrum of the model complex [51]. The insets show expanded views of the $1s \rightarrow 3d$ pre-edge region and first derivatives of the experimental (solid line) and the calculated (dotted line) data.

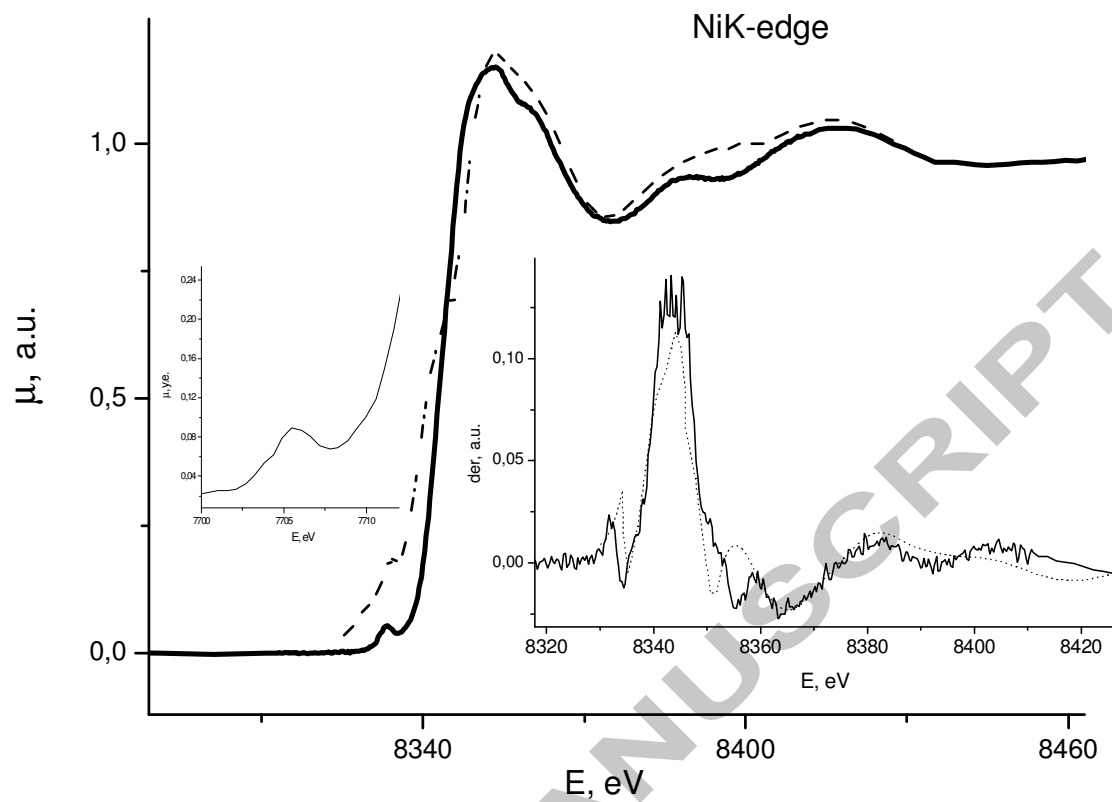


Fig. 4. The experimental Ni *K*-edge XAS spectrum (solid line) of **3b(Ni)** complex and calculated NiK-edge XAS spectrum (dashed line) of model complex [52]. The insets show expanded views of the $1s \rightarrow 3d$ pre-edge region and first derivatives of the experimental (solid line) and the calculated (dotted line) data.

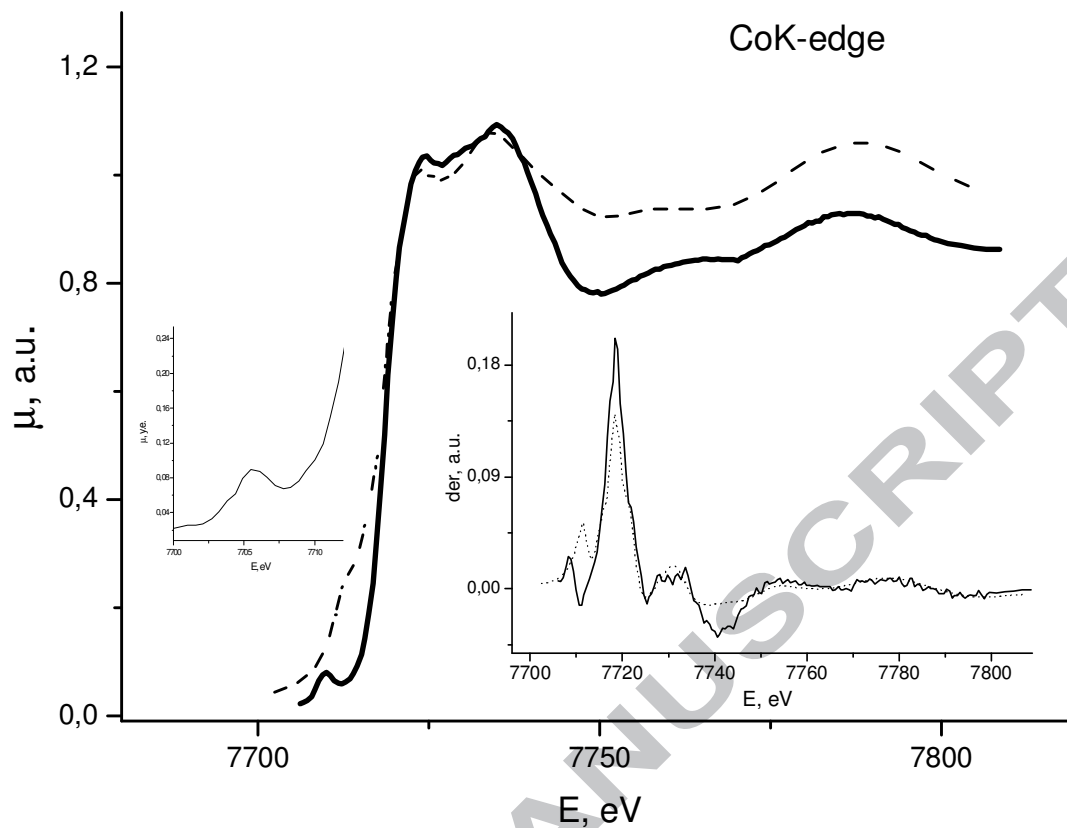


Fig. 5. The experimental Co *K*-edge XAS spectrum (solid line) of **3a**(Co) complex and calculated Co *K*-edge XAS spectrum (dashed line) of model complex [53]. The insets show expanded views of the 1s→3d pre-edge region and first derivatives of the experimental (solid line) and the calculated (dotted line) data.

3.2.4. EXAFS measurements

The EXAFS provides direct, local structural information about the atomic surrounding of the metal being probed. The magnitude of Fourier transforms (MFT) of k^3 -weighted experimental and simulated EXAFS data of the Cu, Ni, and Co *K*-edges for **3(a,b,c)** complexes are presented in Fig. 6. A comparison of these MFT reveals that they are almost identical, suggesting strong similarities in the geometry around the metal ions. There is an intense major peak at $r = 1.52$ - 1.56 Å and several minor peaks at longer distances. The first peak of MFT is associated to the nearest-neighbor scattering from the coordinated nitrogen atoms of the azomethine ligands. The longer-distance

backscattering peaks arise partly from the more distant carbon atoms of the azomethine ligands as well as sulfur atoms and coordinated oxygen atoms of the tosylamine fragments. The suggestion that the oxygen atoms of the tosylamine fragments are coordinated in the metal complexes can be derived from analysis of similar structures [51-53] retrieved from CSD.

Curve-fitting for the three spectra was performed on filtered first-shell and more distant shells contributions of S and O atoms of the tosylamine fragments. Fitting results (bond distances R , coordination numbers N , and Debye-Waller factors σ^2) for the metal nearest neighbor environment are listed in Table 2. All three complexes have a nitrogen nearest neighbor shell at average distances from 1.96 Å for **3c** to 2.01 Å for **3b** and intermediate value 2.00 Å for **3a**. The use of two non-equivalent M-N distances for **3b** greatly improved the fit. In all cases the coordination number for the first shell was equal to four, indicating the tetrahedral donor environment of central metal atoms. The relatively large Debye-Waller factor for first shell in **3c** indicates the disorder in the metal-ligand bond lengths in this complex.

The outer-shells for all complexes **3(a,b,c)** were modeled with sulfur and oxygen atoms of the tosylamine fragments. The best-fit model for these complexes was built using only one oxygen atom and one sulfur atom from both tosylamine groups. The $M\cdots O(Ts)$ distances in complexes **3(a,b,c)** are significantly different and they depend on the metal type forming a series $Cu\cdots O(Ts) < Ni\cdots O(Ts) < Co\cdots O(Ts)$ (see Table 2).

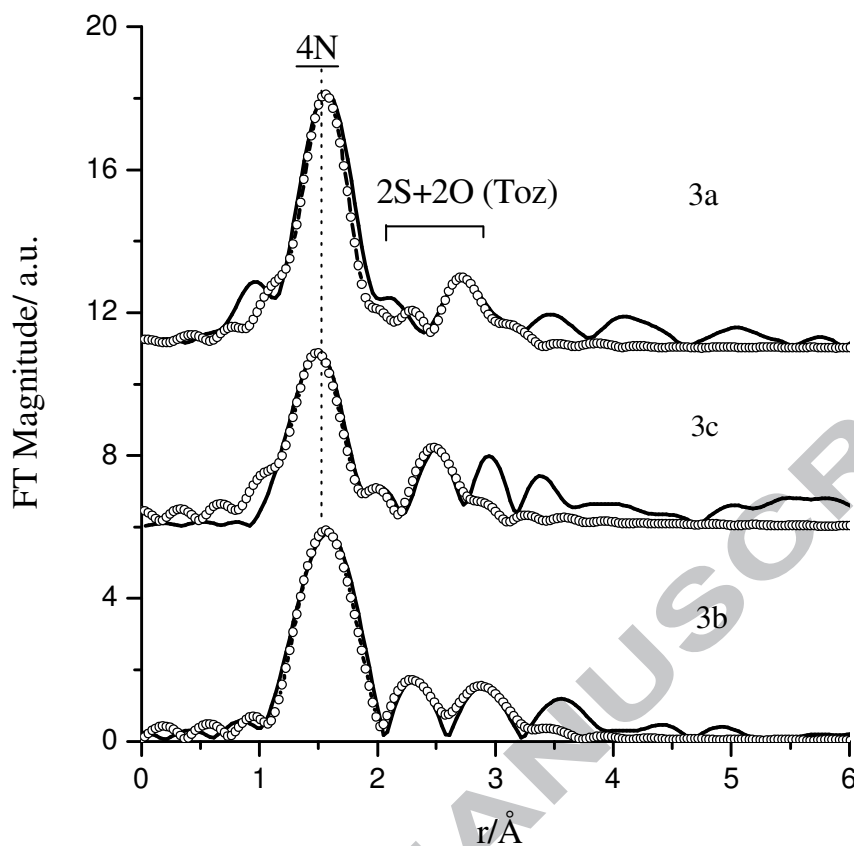


Fig. 6. Magnitudes of Fourier transforms of k^3 -weighted EXAFS of the Cu, Ni, and Co K -edges for **3(a,b,c)** complexes. The open cycles show the best fits.

Table 2

Curve fitting results for EXAFS of the **3(a,b,c)** complexes (R is the metal–scatterer distance, N - the number of scatterers, σ^2 is a mean–square displacement in R , Q - the goodness-of-fit parameter, Δ is an interligand tilt angle).

Compound	N	R , \AA	σ^2 , \AA^2	Δ , degree	Scattering atom	Q , %
	4	2.00	0.0037		N	

3a	2	2.90	0.0040	51	O(Ts)	4.3
	2	3.08	0.0055		S(Ts)	
3b	2	2.01	0.0038	16	N	5.6
	2	1.96	0.0038		N	
	2	2.76	0.0050		O(Ts)	
	2	2.93	0.0060		S(Ts)	
3c	4	1.96	0.0053	56	N	4.7
	2	2.56	0.0045		O(Ts)	
	2	2.88	0.0045		S(Ts)	

4. Conclusions

The four metal chelates (Co^{2+} , Ni^{2+} , Cu^{2+} , and Zn^{2+}) on the base of azomethine of *o*-tosylaminobenzaldehyde and *p*-aminoazobenzene (**2**) was synthesized and investigated by IR, ^1H NMR spectroscopy, XAFS, and magnetic measurements. X-ray data for ligand **2** showed that the azomethine exists in the amino-imine tautomeric form both in solutions and solid state. XAFS investigations revealed that the complexes adopt either distorted tetrahedral or octahedral donor environment that was in accordance with magnetochemical data.

Acknowledgments

This investigation was performed with the financial support of the grant of Russian Found for Basic Researches (grants 11-03-00475, 12-03-00462 and 13-03-00171) and Ministry of Education and Science of Russian Federation (grant NS-927.2012.3).

ACCEPTED MANUSCRIPT

References

- [1] R. Hernandez Molina, A. Mederos. In: *Comprehensive Coordination Chemistry II*, A.B.P. Lever (Ed.), vol. 1, p. 411, Elsevier – Pergamon Press, Amsterdam – Oxford – New York (2003).
- [2] A.D. Garnovskii, B.I. Kharissov (Eds.) *Synthetic Coordination and Organometallic Chemistry*, Marcel Dekker, New York – Basel, 513 p. (2003).
- [3] P.A. Vigato, S. Tamburini. *Coord. Chem. Rev.* 248 (2004) 1717.
- [4] P.A. Vigato, S. Tamburini, L. Bertelo. *Coord. Chem. Rev.* 251 (2007) 1311.
- [5] P.A. Vigato, S. Tamburini, L. Bertelo. *Coord. Chem. Rev.* 252 (2008) 1871.
- [6] A.D. Garnovskii, I.S. Vasilchenko. *Russ. Chem. Rev.* 71 (2002) 943.
- [7] A.D. Garnovskii, I.S. Vasilchenko. *Russ. Chem. Rev.* 74 (2005) 193.
- [8] A.D. Garnovskii, I.S. Vasilchenko, D.A. Garnovskii, B.I. Kharisov. *J. Coord. Chem.* 62 (2009) 151.
- [9] A.D. Garnovskii, A.P. Sadimenko, I.S. Vasilchenko, D.A. Garnovskii, E.V. Sennikova, V.I. Minkin. *Adv. Heterocycl. Chem.* 97, (2009) 291.
- [10] D.J. Darensbourg, R.M. Mackiewicz, A.L. Phelps, D.R. Billodeaux. *Acc. Chem. Res.* 37 (2004) 836.
- [11] H. Miyasaka, A. Saitoh, S. Abe. *Coord. Chem. Rev.* 251 (2007) 2622.
- [12] K.S. Gupta, A.K. Sutar. *Coord. Chem. Rev.* 252 (2008) 1420.
- [13] A.D. Garnovskii, V.N. Ikorskii, A.I. Uraev, I.S. Vasilchenko, A.S. Burlov, D.A. Garnovskii, K.A. Lyssenko, V.G. Vlasenko, T.E. Shestakova, Y.V. Koshchienko, T.A. Kuz'menko, L.N. Divaeva, M.P. Bubnov, V.P. Rybalkin, O.Yu. Korshunov, I.V. Pirog, G.S. Borodkin, V.A. Bren, I.E. Uflyand, M.Yu. Antipin, V.I. Minkin. *J. Coord. Chem.* 60 (2007) 1493.

- [14] A.D. Garnovskii, I.S. Vasilchenko, D.A. Garnovskii, A.S. Burlov, A.I. Uraev. *Mendeleev Chem. J. (Rus.)* 53 (2009) 100.
- [15] A. S. Burlov, S. A. Nikolaevskii, A. S. Bogomyakov, I. S. Vasil'chenko, Yu. V. Koshchienko, V. G. Vlasenko, A. I. Uraev, D. A. Garnovskii, E. V. Sennikova, G. S. Borodkin, A. D. Garnovskii, and V. I. Minkin. *Russ. J. Coord. Chem.* 35 (2009) 486.
- [16] X.-M. Li, C.-F. Wang, J.-L. Zuo, X.-Z. You. *J. Coord. Chem.* 62 (2009) 1544.
- [17] A.V. Metelitsa, A.S. Burlov, S.O. Bezugly, I.G. Borodkina, V.A. Bren, A.D. Garnovskii, V.I. Minkin. *Russ. J. Coord. Chem.* 32 (2006) 858.
- [18] L. Zhang, F. Jiang, Yu. Zhou. *J. Coord. Chem.* 62 (2009) 1476.
- [19] R.H. Holm, E.I. Solomon (Guest Eds.), *Chem. Rev.* 104 (2004) 347-1200 (the whole issue).
- [20] F.T. Elmali, A. Peksel, N. Demizhan. *J. Coord. Chem.* 62 (2009) 2548.
- [21] A.D. Garnovskii, A.S. Burlov, A.G. Starikov, A.V. Metelitsa, I.S. Vasilchenko, S.O. Bezuglyi, S.A. Nikolaevskii, I.G. Borodkina, V.I. Minkin. *Russ. J. Coord. Chem.* 36 (2010) 483.
- [22] I. Aiello, M. Ghedini, F. Neve, D. Pucci. *Chem. Mater.* 9 (1997) 2107.
- [23] A.A. Khandar, Z. Rezvani. *Polyhedron.* 18 (1999) 129.
- [24] Z. Rezvani, M.A. Ghanea, K. Nejati, S. A. Baghaei. *Polyhedron.* 28, (2009) 2913.
- [25] L.C. Visentin, L.C. Ferreira, J. Bordinhao, C.A.L. Filgueiras. *J. Braz. Chem. Soc.* 21 (2010) 1187.
- [26] N. Chopin, M. Medebielle, G. Pilet. *Eur. J. Inorg. Chem.* (2012) 1093.
- [27] G.M. Sheldrick. *SHELXTL PLUS, PC Version, a. System of Computer Programs for the Determination of Crystal Structure from X-ray Diffraction Data, Rev. 502*, Siemens Analytical X-Ray Instruments Inc., Germany, 1994.

- [28] A.A. Chernyshov, A.A. Veligzhanin, Y.V. Zubavichus. Nucl. Instr. Meth. Phys. Res. A. 603 (2009) 95.
- [29] M. Newville. J.Synchrotron Rad. 8 (2001) 322.
- [30] S.I. Zabinski, J.J. Rehr, A. Ankudinov, R.C. Albers, M.J. Eller. Phys.Rev. B. 52 (1995) 2995.
- [31] A.E. Obodovskaya, Z.A. Starikova, V.K. Trunov, B.M. Bolotin. Zh. Strukt. Khim. (Russ.), (J. Struct. Chem.). 22 (1981) 104.
- [32] A.S. Antsyshkina, G.G. Sadikov, A.S. Burlov, E.L. Koroleva, D.A. Garnovskii, I.S. Vasil'chenko, I.F. Uflyand, V.S. Sergienko, A.D. Garnovskii. Koord. Khim. (Russ.), (Coord.Chem.). 26 (2000) 779.
- [33] J. Mahia, M.A. Maestro, M. Vazquez, M.R. Bermejo, A.M. Gonzalez, M.Maneiro. Acta Crystallogr., Sect. C: Cryst. Struct. Commun. 56 (2000) 492.
- [34] L.Kh. Minacheva, I.S. Ivanova, A.V. Dorokhov, A.V. Bicherov, A.S. Burlov, A.D. Garnovskii, V.S. Sergienko, A.Yu. Tsivadze. Dokl. Akad. Nauk (Russ.), (Proc. Nat. Acad. Sci.). 398, (2004) 62.
- [35] M. Morioca, M. Kato, H. Yoshida, T. Ogata. Heterocycles. 45 (1999) 1229.
- [36] K. Nakamoto in *Infrared and Raman Spectra of Inorganic and Coordination Compounds*, John Wiley & Sons, New York, 1997.
- [37] M. Vazquez, M.R. Bermejo, M. Fondo, A. Garcia-Deibe, A.M. Gonzalez, R. Pedrido. Eur. J. Inorg. Chem. (2002) 465.
- [38] M. Vazquez, M.R. Bermejo, M. Fondo, A. Garcia-Deibe, A.M. Gonzalez, R. Pedrido, J. Sanmartin. Z. Anorg. Allg. Chem. 628 (2002) 1068.
- [39] F.H. Allen, O. Kennard, D.G. Watson, L. Brammer, A.G. Orpen, R. Taylor. J. Chem. Soc., Perkin Trans. 2. (1987) S1.
- [40] T. Steiner. Crystallogr. Rev. 9 (2003) 177.

- [41] A. Sousa-Pedrares, J.A. Viqueira, J. Antelo, E. Labisbal, J. Romero, A. Sousa, O.R. Nascimento, J. Garcia-Vazquez. *Eur. J. Inorg. Chem.* (2011) 2273.
- [42] R.G. Shulman, T. Yafet, P. Eisenberger, W.E. Blumberg. *Proc. Nat. Acad. Sci. U.S.A.* 73 (1976) 1384.
- [43] J.E. Hahn, R.A. Scott, K.O. Hodgson, S. Doniach, S.E. Desjardins, E.I. Solomon. *Chem. Phys. Lett.* 88 (1982) 595.
- [44] T.E. Westre, P. Kennepohl, J.G. DeWitt, B. Hedman, K.O. Hodgson, E.I. Solomon. *J. Am. Chem. Soc.* 119 (1997) 6297.
- [45] T.A. Smith, M. Berding, J.E. Penner-Hahn, S. Doniach, K.O. Hodgson. *J. Am. Chem. Soc.* 107 (1985) 5945.
- [46] R.A. Blair, W.A. Goddard. *Phys. Rev., B.* 22 (1980) 2767.
- [47] N. Kosugi, T. Yokoyama, K. Asakuna, H. Kuroda. *Proc. Phys.* 2 (1984) 55.
- [48] A.L. Ankudinov, B. Ravel, J.J. Rehr, S.D. Conradson. *Phys. Rev. B.* 58 (1998) 7565.
- [49] A.L. Ankudinov, C.E. Bouldin, J.J. Rehr, J. Sims, H. Hung. *Phys. Rev. B.* 65 (2002) 104107.
- [50] A.V. Soldatov, A.N. Kravtsova, L.N. Mazalov, S.V. Trubina, N.A. Kryuchkova, G.B. Sukharina. *Rus. J. Struct. Chem.* 48 (2007) 1061.
- [51] M. Vazquez, M.R. Bermejo, M. Fondo, A.M. Garcia-Deibe, J. Sanmartin, R. Pedrido, L. Sorace, D. Gatteschi. *Eur. J. Inorg. Chem.* (2003) 1128.
- [52] M. Vazquez, M.R. Bermejo, J. Sanmartin, A.M. Garcia-Deibe, C. Lodeiro, J. Mahia. *J. Chem. Soc., Dalton Trans.* (2002) 870.
- [53] I. Karame, M.L. Tommasino, R. Faure, M. Lemaire. *Eur. J. Org. Chem.* (2003) 1271.

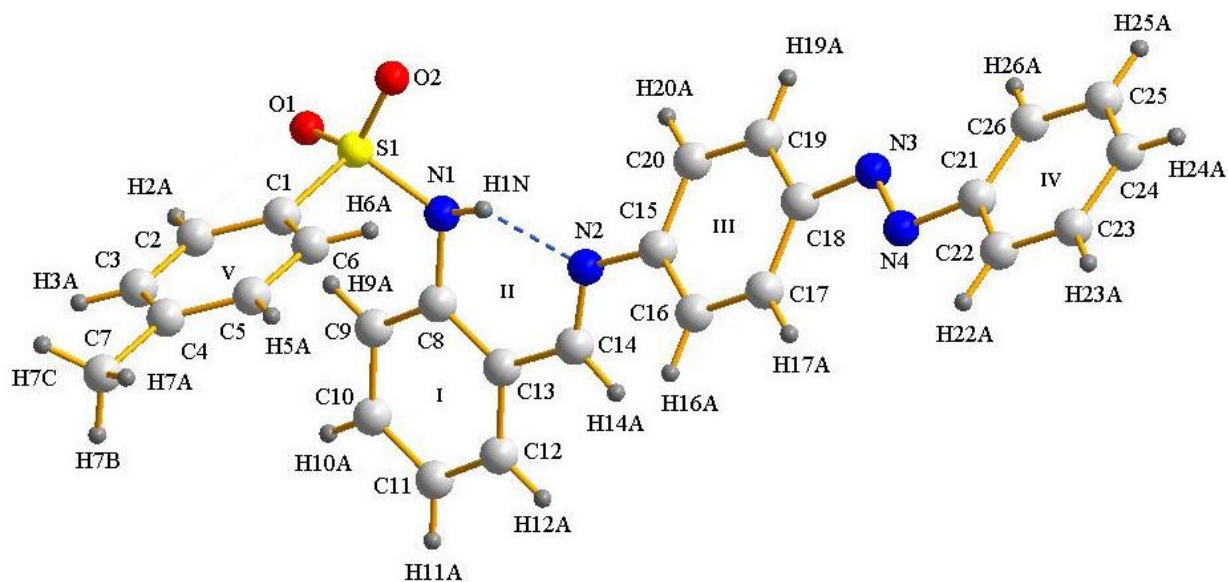


Fig. 1. Structure of the azomethine **2**. Selected bond distances (Å): S(1)-O(1) 1.4282(18), S(1)-O(2) 1.4349(18), S(1)-N(1) 1.630(2), S(1)-C(1) 1.759(2), N(1)-C(8) 1.412(3), N(1)-H(1)N 0.9121, N(2)-C(14) 1.279(3), N(2)-C(15) 1.413(3), N(3)-N(4) 1.261(3), N(3)-C(18) 1.422(3), N(4)-C(21) 1.425(3); and valence angles (°): O(1)S(1)O(2) 119.43(11), O(1)S(1)N(1) 109.91(11), O(2)S(1)N(1) 104.06(10), O(1)S(1)C(1) 107.02(11), O(2)S(1)C(1) 109.19(12), N(1)S(1)C(1) 106.59(11), C(8)N(1)S(1) 125.30(16), C(8)N(1)H(1)N 111.5, S(1)N(1)H(1)N 108.7, C(14)N(2)C(15) 121.5(2), N(4)N(3)C(18) 114.2(2), N(3)N(4)C(21) 113.7(2).

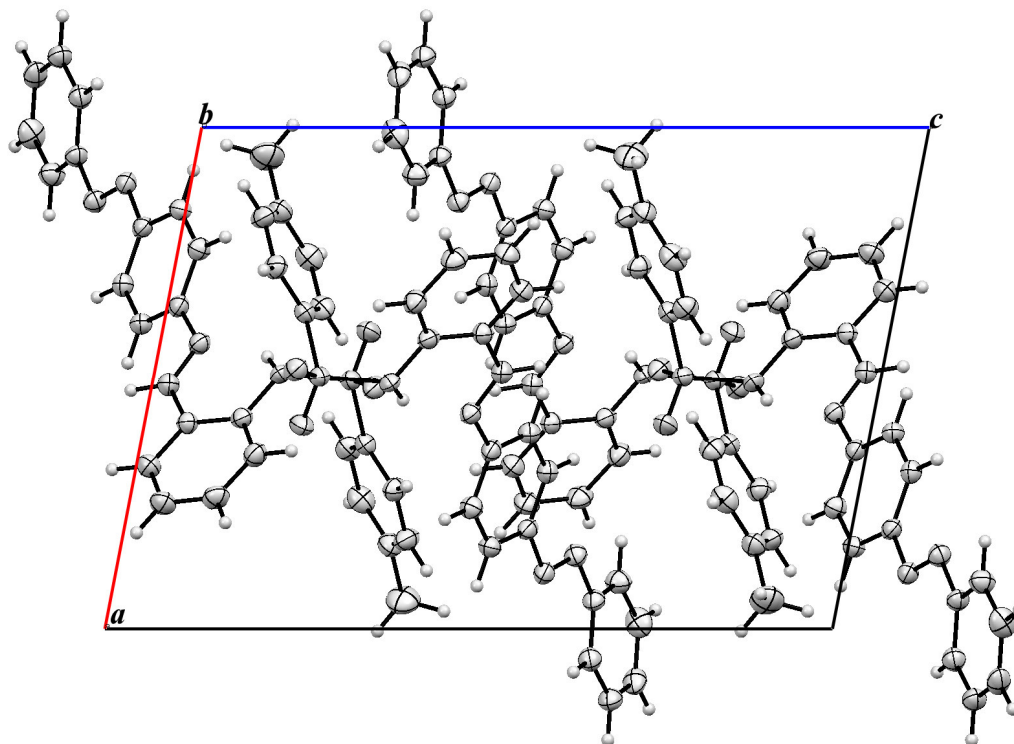


Fig. 2. View of crystal packing of **2** along *b* crystallographic axis.

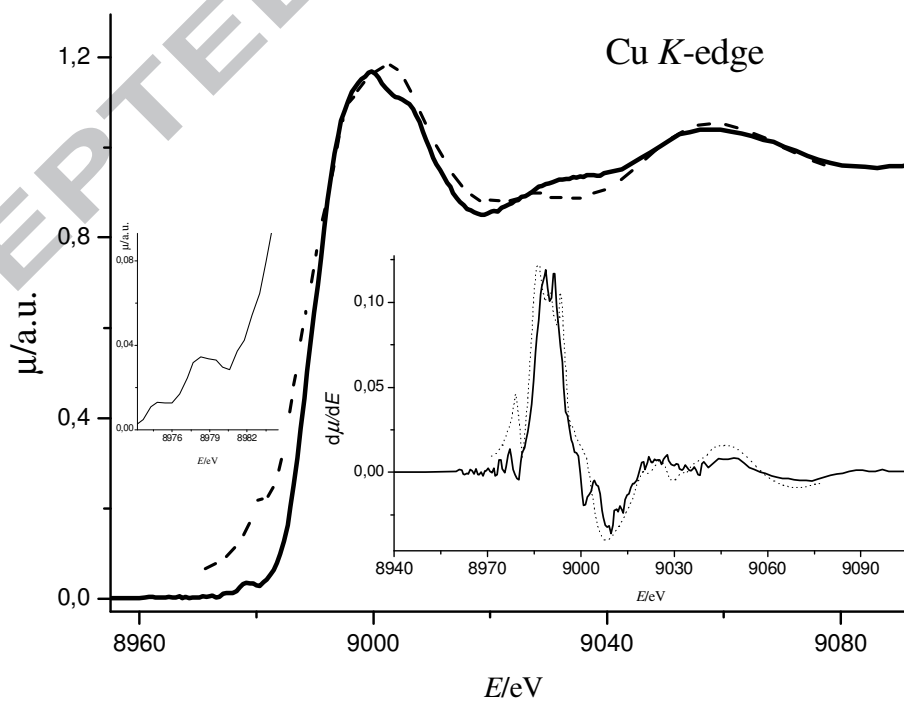


Fig. 3. The experimental Cu *K*-edge XAS spectrum (solid line) of **3c** complex and calculated Cu*K*-edge (dashed line) XAS spectrum of the model complex [51]. The insets show expanded views of the 1s→3d pre-edge region and first derivatives of the experimental (solid line) and the calculated (dotted line) data.

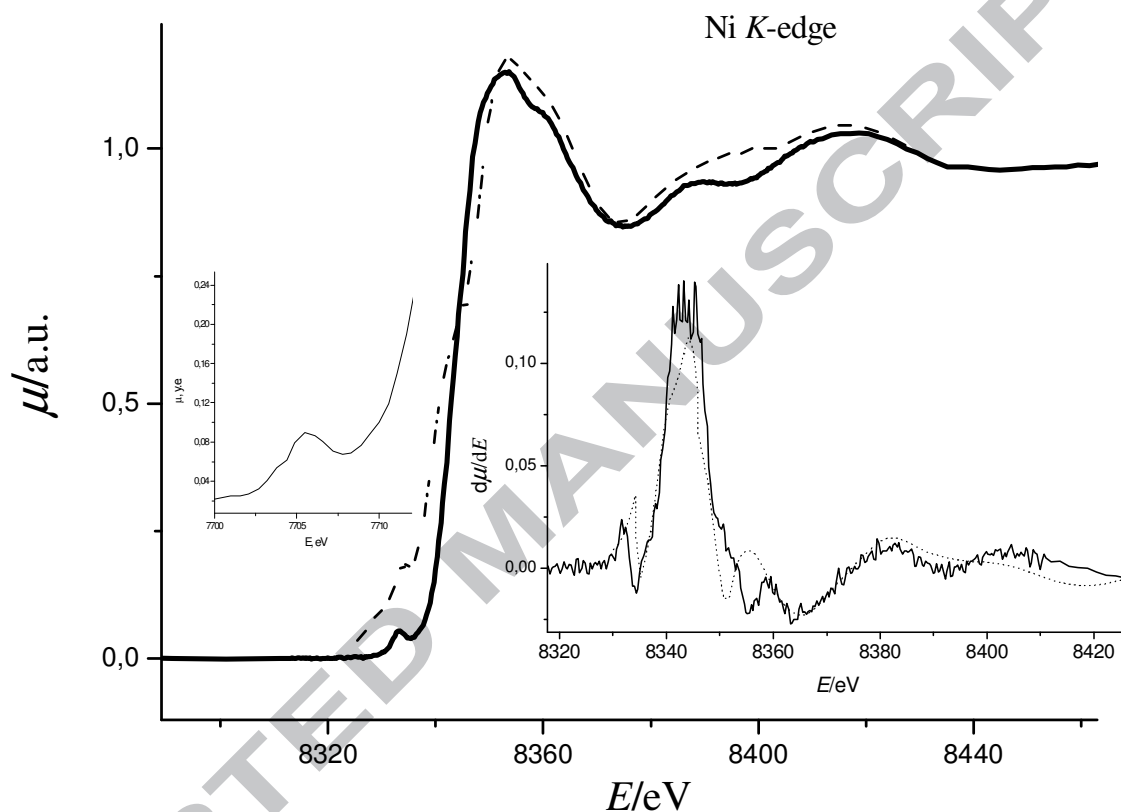


Fig. 4. The experimental Ni *K*-edge XAS spectrum (solid line) of **3b**(Ni) complex and calculated Ni*K*-edge XAS spectrum (dashed line) of model complex [52]. The insets show expanded views of the 1s→3d pre-edge region and first derivatives of the experimental (solid line) and the calculated (dotted line) data.

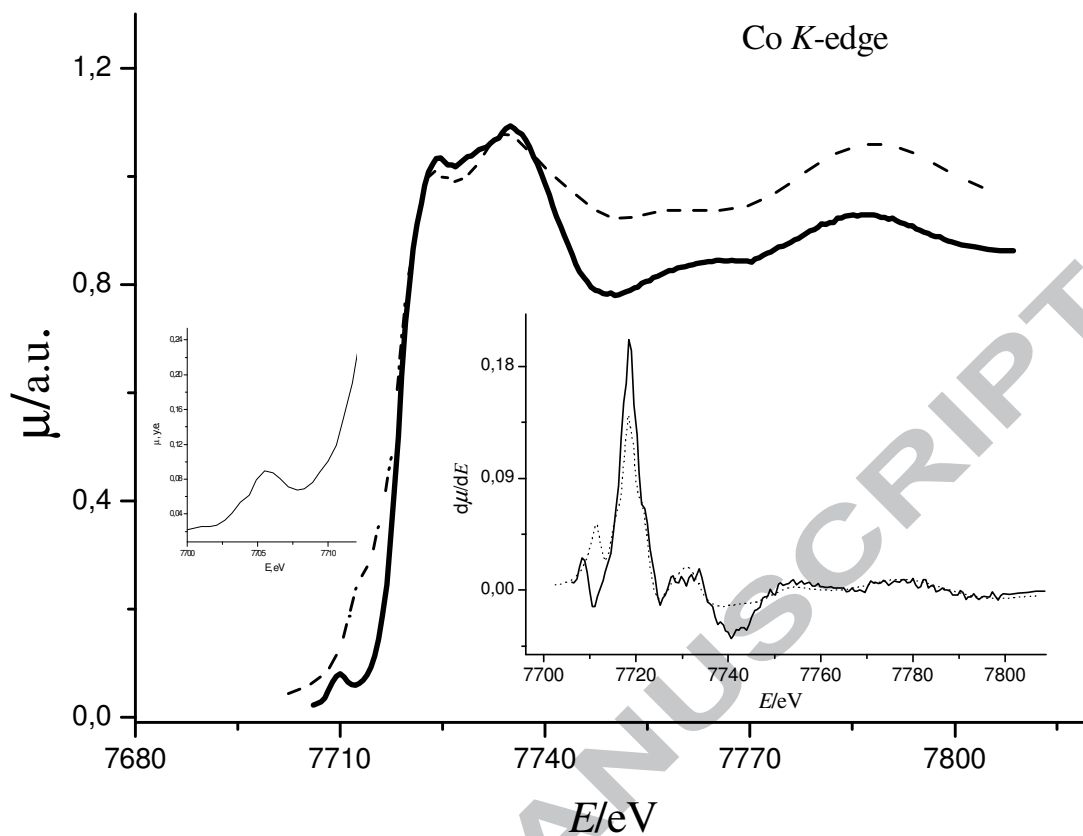


Fig. 5. The experimental Co *K*-edge XAS spectrum (solid line) of **3a**(Co) complex and calculated Co*K*-edge XAS spectrum (dashed line) of model complex [53]. The insets show expanded views of the 1s→3d pre-edge region and first derivatives of the experimental (solid line) and the calculated (dotted line) data.

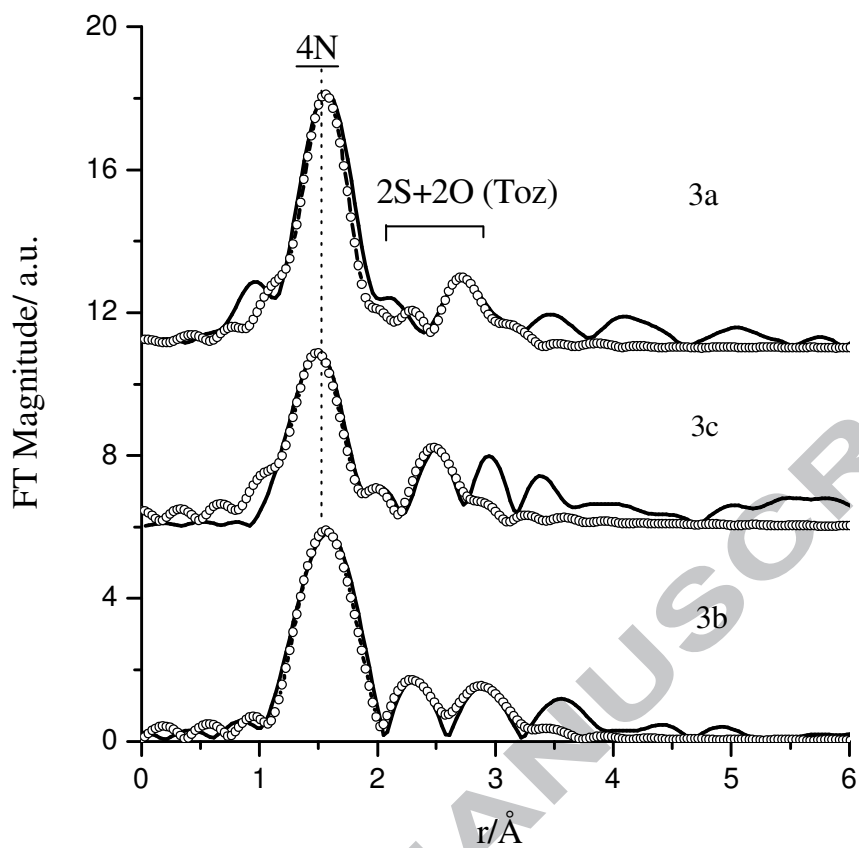


Fig. 6. Magnitudes of Fourier transforms of k^3 -weighted EXAFS of the Cu, Ni, and Co K -edges for **3(a,b,c)** complexes. The open cycles show the best fits.

Table 1. Characteristics of hydrogen bonds in the crystal of compound **2**

D–H...A	D– H, Å	H...A, Å	D...A, Å	∠DHA, deg.
N(1)–H(1N)...N(2)	0.91	1.88	2.656(3)	142
C(2)–H(2A)...O(1)	0.95	2.49	2.872(3)	104
C(9)–H(9A)...O(1)	0.95	2.51	3.164(3)	126
C(6)–H(6A)...O(1) ⁱ	0.95	2.35	3.216(3)	151
C(25)– H(25A)...O(2) ⁱⁱ	0.95	2.47	3.234(3)	138

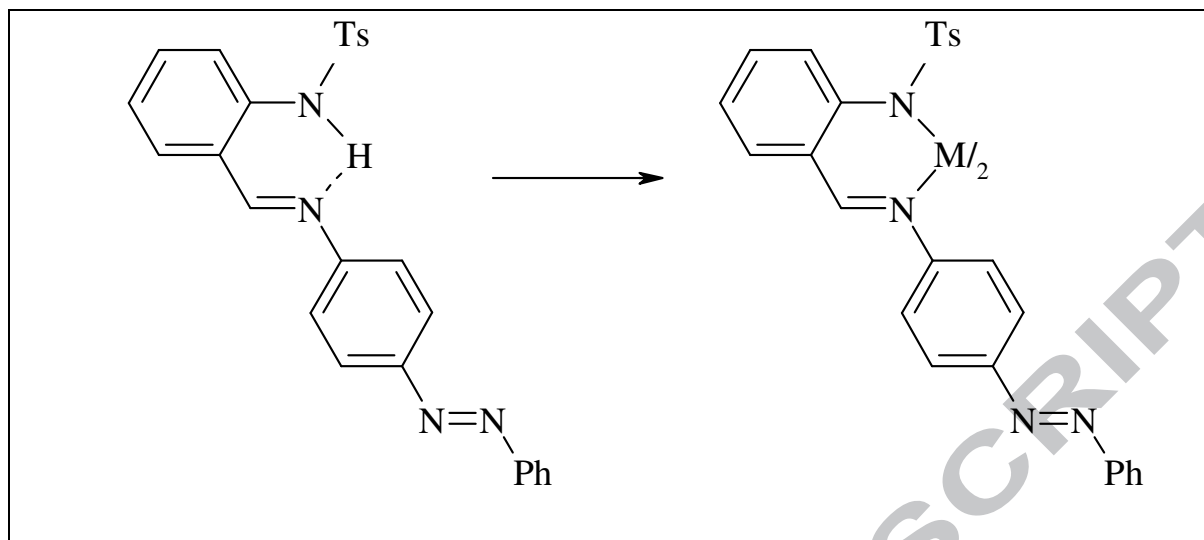
Crystallographic sites: (i) 2–x, 1–y, 1–z; (ii) 1–x, 1/2+y, 1/2–z.

Table 2. Curve fitting results for EXAFS of the **3(a,b,c)** complexes (R is the metal–scatterer distance, *N* - the number of scatterers, σ^2 is a mean–square displacement in R, *Q*- the goodness-of-fit parameter, Δ is an interligand tilt angle).

compound	<i>N</i>	R, Å	$\sigma^2, \text{Å}^2$	Δ , degree	scattering atom	<i>Q</i> , %
3a	4	2.00	0.0037	51	N	4.3
	2	2.90	0.0040		O(Ts)	
	2	3.08	0.0055		S(Ts)	
	2	2.01	0.0038	16	N	5.6
	2	1.96	0.0038		N	

3b	2	2.76	0.0050		O(Ts)	
	2	2.93	0.0060		S(Ts)	
3c	4	1.96	0.0053		N	
	2	2.56	0.0045	56	O(Ts)	4.7
	2	2.88	0.0045		S(Ts)	

ACCEPTED MANUSCRIPT



ACCEPTED MANUSCRIPT

HIGHLIGHTS

- Four complexes (**3a-d**) synthesized on the base of bidentate *N,N*-ligand **2** derived from *o*-tosylaminobenzaldehyde and *p*-aminoazobenzene.
- The structure of imine **2** was determined by X-ray crystallography.
- Parameters and geometry of the local donor environment for **3a-c** were established by XAFS.

ACCEPTED MANUSCRIPT